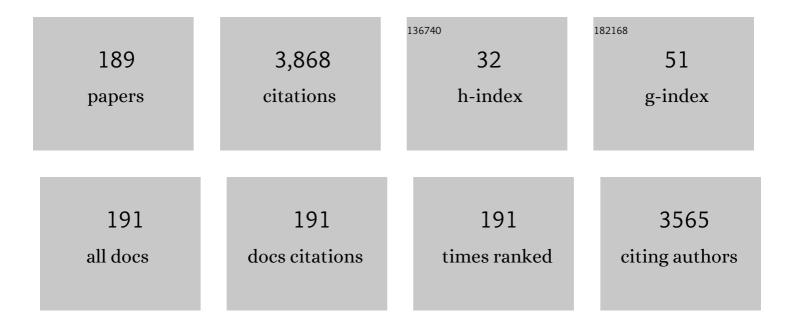
## Florinda Costa

List of Publications by Year in descending order

Source: https://exaly.com/author-pdf/1787040/publications.pdf Version: 2024-02-01



#	Article	IF	CITATIONS
1	A critical review on the production and application of graphene and graphene-based materials in anti-corrosion coatings. Critical Reviews in Solid State and Materials Sciences, 2022, 47, 309-355.	6.8	45
2	A Review on the Applications of Graphene in Mechanical Transduction. Advanced Materials, 2022, 34, e2101326.	11.1	59
3	Laserâ€Induced Graphene from Paper by Ultraviolet Irradiation: Humidity and Temperature Sensors. Advanced Materials Technologies, 2022, 7, .	3.0	39
4	Label-Free Nanoscale ZnO Tetrapod-Based Transducers for Tetracycline Detection. ACS Applied Nano Materials, 2022, 5, 1232-1243.	2.4	5
5	ZnO Transducers for Photoluminescence-Based Biosensors: A Review. Chemosensors, 2022, 10, 39.	1.8	12
6	Conversion of paper and xylan into laser-induced graphene for environmentally friendly sensors. Diamond and Related Materials, 2022, 123, 108855.	1.8	20
7	Optical Studies in Red/NIR Persistent Luminescent Cr-Doped Zinc Gallogermanate (ZGGO:Cr). Applied Sciences (Switzerland), 2022, 12, 2104.	1.3	3
8	Relevance of the Spectral Analysis Method of Tilted Fiber Bragg Grating-Based Biosensors: A Case-Study for Heart Failure Monitoring. Sensors, 2022, 22, 2141.	2.1	4
9	Label-free plasmonic immunosensor for cortisol detection in a D-shaped optical fiber. Biomedical Optics Express, 2022, 13, 3259.	1.5	73
10	Laser-induced graphene from paper for non-enzymatic uric acid electrochemical sensing in urine. Carbon, 2022, 197, 253-263.	5.4	32
11	Laser-Induced Graphene from Paper for Mechanical Sensing. ACS Applied Materials & Interfaces, 2021, 13, 10210-10221.	4.0	115
12	Cortisol AuPd plasmonic unclad POF biosensor. Biotechnology Reports (Amsterdam, Netherlands), 2021, 29, e00587.	2.1	76
13	IR and UV Laserâ€Induced Graphene: Application as Dopamine Electrochemical Sensors. Advanced Materials Technologies, 2021, 6, 2100007.	3.0	58
14	Dual Transduction of H2O2 Detection Using ZnO/Laser-Induced Graphene Composites. Chemosensors, 2021, 9, 102.	1.8	13
15	Electrochemical Response of Glucose Oxidase Adsorbed on Laser-Induced Graphene. Nanomaterials, 2021, 11, 1893.	1.9	17
16	Electrochemical and photoluminescence response of laser-induced graphene/electrodeposited ZnO composites. Scientific Reports, 2021, 11, 17154.	1.6	13
17	Immunosensing Based on Optical Fiber Technology: Recent Advances. Biosensors, 2021, 11, 305.	2.3	83
18	Laser Floating Zone Growth: Overview, Singular Materials, Broad Applications, and Future Perspectives. Crystals, 2021, 11, 38.	1.0	11

#	Article	IF	CITATIONS
19	Laser floating zone growth of Yb, or Nd, doped (Lu <sub>0.3</sub> Gd <sub>0.7</sub> ) <sub>2</sub> SiO <sub>5</sub> oxyorthosilicate single-crystal rods with efficient laser performance. Journal of Materials Chemistry C, 2020, 8, 2065-2073.	2.7	11
20	Millimeter-sized few-layer suspended graphene membranes. Applied Materials Today, 2020, 21, 100879.	2.3	14
21	Laser Floating Zone: General Overview Focusing on the Oxyorthosilicates Growth. , 2020, , .		3
22	Millimeter sized graphene domains through in situ oxidation/reduction treatment of the copper substrate. Carbon, 2020, 169, 403-415.	5.4	8
23	Cortisol in-fiber ultrasensitive plasmonic immunosensing. IEEE Sensors Journal, 2020, , 1-1.	2.4	49
24	Laserâ€Induced Graphene Piezoresistive Sensors Synthesized Directly on Cork Insoles for Gait Analysis. Advanced Materials Technologies, 2020, 5, 2000630.	3.0	53
25	Laser-Induced Hematite/Magnetite Phase Transformation. Journal of Electronic Materials, 2020, 49, 7187-7193.	1.0	8
26	Nd:YAG laser scribed zinc oxide on semi-flexible copper foils. Materials Letters: X, 2020, 5, 100038.	0.3	0
27	Influence of laser structural patterning on the tribological performance of C-alloyed W-S coatings. Surface and Coatings Technology, 2020, 394, 125822.	2.2	9
28	ZnO decorated laser-induced graphene produced by direct laser scribing. Nanoscale Advances, 2019, 1, 3252-3268.	2.2	23
29	Physical Structure and Electrochemical Response of Diamond–Graphite Nanoplatelets: From CVD Synthesis to Label-Free Biosensors. ACS Applied Materials & Interfaces, 2019, 11, 8470-8482.	4.0	16
30	A review on the laser-assisted flow deposition method: growth of ZnO micro and nanostructures. CrystEngComm, 2019, 21, 1071-1090.	1.3	23
31	Intense red emission on dilute Mn-doped CaYAlO4-based ceramics obtained by laser floating zone. Journal of Materials Science: Materials in Electronics, 2019, 30, 21454-21464.	1.1	2
32	Insights into the photoluminescence properties of gel-like carbon quantum dots embedded in poly(methyl methacrylate) polymer. Materials Today Communications, 2019, 18, 32-38.	0.9	11
33	Improvement of thermoelectric properties of Ca0.9Gd0.1MnO3 by powder engineering through K2CO3 additions. Journal of Materials Science, 2019, 54, 3252-3261.	1.7	4
34	Molecularly-imprinted chloramphenicol sensor with laser-induced graphene electrodes. Biosensors and Bioelectronics, 2019, 124-125, 167-175.	5.3	135
35	Unusual redox behaviour of the magnetite/hematite core–shell structures processed by the laser floating zone method. Dalton Transactions, 2018, 47, 5646-5651.	1.6	10
36	Shifting Lu2SiO5 crystal to eutectic structure by laser floating zone. Journal of the European Ceramic Society, 2018, 38, 2059-2067.	2.8	13

#	Article	IF	CITATIONS
37	New environmentally friendly Ba-Fe-O thermoelectric material by flexible laser floating zone processing. Scripta Materialia, 2018, 145, 54-57.	2.6	7
38	(Lu <sub>0.3</sub> Gd <sub>0.7</sub> ) <sub>2</sub> SiO <sub>5</sub> :Y <sup>3+</sup> single crystals grown by the laser floating zone method: structural and optical studies. CrystEngComm, 2018, 20, 7386-7394.	1.3	11
39	Laserâ€Induced Graphene Strain Sensors Produced by Ultraviolet Irradiation of Polyimide. Advanced Functional Materials, 2018, 28, 1805271.	7.8	228
40	Photocatalytic Activity of Laserâ€Processed ZnO Micro/Nanocrystals. Physica Status Solidi (A) Applications and Materials Science, 2018, 215, 1800155.	0.8	14
41	Structural and redox effects in iron-doped magnesium aluminosilicates. Journal of Crystal Growth, 2017, 457, 19-23.	0.7	3
42	Diamond-Graphite Nanoplatelet Surfaces as Conductive Substrates for the Electrical Stimulation of Cell Functions. ACS Applied Materials & amp; Interfaces, 2017, 9, 1331-1342.	4.0	18
43	Exploring the effects of silica and zirconia additives on electrical and redox properties of ferrospinels. Journal of the European Ceramic Society, 2017, 37, 2621-2628.	2.8	2
44	Tuning the field emission of graphene-diamond hybrids by pulsed methane flow CVD. Carbon, 2017, 122, 726-736.	5.4	15
45	Effect of laser irradiation on lithium niobate powders. Ceramics International, 2017, 43, 2504-2510.	2.3	6
46	A mixture toxicity approach to predict the toxicity of Ag decorated ZnO nanomaterials. Science of the Total Environment, 2017, 579, 337-344.	3.9	25
47	Structural and optical characterization of Gd_2SiO_5 crystalline fibres obtained by laser floating zone. Optical Materials Express, 2017, 7, 868.	1.6	14
48	Processing Effects on Properties of (Fe,Mg,Al) <sub>3</sub> O <sub>4</sub> Spinels as Potential Consumable Anodes for Pyroelectrolysis. Journal of the American Ceramic Society, 2016, 99, 1889-1893.	1.9	6
49	Structural, optical, and electrical properties of SmNbO4. Journal of Applied Physics, 2016, 120, .	1.1	13
50	A new concept of ceramic consumable anode for iron pyroelectrolysis in magnesium aluminosilicate melts. Ceramics International, 2016, 42, 11070-11076.	2.3	9
51	Correction to "Spectroscopic Analysis of Eu <sup>3+</sup> Implanted and Annealed GaN Layers and Nanowires― Journal of Physical Chemistry C, 2016, 120, 6907-6908.	1.5	5
52	Exploring the potential of laser assisted flow deposition grown ZnO for photovoltaic applications. Materials Chemistry and Physics, 2016, 177, 322-329.	2.0	18
53	Tailoring Ca3Co4O9 microstructure and performances using a transient liquid phase sintering additive. Journal of the European Ceramic Society, 2016, 36, 1025-1032.	2.8	38
54	Guidelines to design multicomponent ferrospinels for high-temperature applications. RSC Advances, 2016, 6, 32540-32548.	1.7	6

#	Article	IF	CITATIONS
55	Simultaneous CVD synthesis of graphene-diamond hybrid films. Carbon, 2016, 98, 99-105.	5.4	19
56	lron incorporation into magnesium aluminosilicate glass network under fast laser floating zone processing. Ceramics International, 2016, 42, 2693-2698.	2.3	11
57	Multiferroic interfaces in bismuth ferrite composite fibers grown by laser floating zone technique. Materials and Design, 2016, 90, 829-833.	3.3	6
58	High thermoelectric performance in Bi2-xPbxBa2Co2Oy promoted by directional growth and annealing. Journal of the European Ceramic Society, 2016, 36, 67-74.	2.8	26
59	Defect luminescence in oxides nanocrystals grown by laser assisted techniques. , 2015, , .		2
60	Effect of solvents on ZnO nanostructures synthesized by solvothermal method assisted by microwave radiation: a photocatalytic study. Journal of Materials Science, 2015, 50, 5777-5787.	1.7	105
61	Very Large Superconducting Currents Induced by Growth Tailoring. Crystal Growth and Design, 2015, 15, 2094-2101.	1.4	52
62	Selfâ€Assembled Functionalized Graphene Nanoribbons from Carbon Nanotubes. ChemistryOpen, 2015, 4, 115-119.	0.9	6
63	One-step synthesis of ZnO decorated CNT buckypaper composites and their optical and electrical properties. Materials Science and Engineering B: Solid-State Materials for Advanced Technology, 2015, 195, 38-44.	1.7	23
64	Pressure effects on the dissipative behavior of nanocrystalline diamond microelectromechanical resonators. Journal of Micromechanics and Microengineering, 2015, 25, 025019.	1.5	4
65	High Thermoelectric Performances in Co-oxides Processed by a Laser Floating Zone Technique. Materials Today: Proceedings, 2015, 2, 654-660.	0.9	4
66	Effect of N2 and H2 plasma treatments on band edge emission of ZnO microrods. Scientific Reports, 2015, 5, 10783.	1.6	43
67	Spectroscopic Analysis of Eu <sup>3+</sup> Implanted and Annealed GaN Layers and Nanowires. Journal of Physical Chemistry C, 2015, 119, 17954-17964.	1.5	13
68	Use of laser technology to produce high thermoelectric performances in Bi2Sr2Co1.8Ox. Materials & Design, 2015, 75, 143-148.	5.1	29
69	Luminescence studies on SnO2 and SnO2:Eu nanocrystals grown by laser assisted flow deposition. Physical Chemistry Chemical Physics, 2015, 17, 13512-13519.	1.3	19
70	Tunable green to red ZrO <sub>2</sub> :Er nanophosphors. RSC Advances, 2015, 5, 20138-20147.	1.7	22
71	Heat Dissipation Interfaces Based on Vertically Aligned Diamond/Graphite Nanoplatelets. ACS Applied Materials & Interfaces, 2015, 7, 24772-24777.	4.0	14
72	Upconversion luminescence and blackbody radiation in tetragonal YSZ co-doped with Tm <sup>3+</sup> and Yb <sup>3+</sup> . Nanoscale, 2015, 7, 19958-19969.	2.8	17

#	Article	IF	CITATIONS
73	Prospects and challenges of iron pyroelectrolysis in magnesium aluminosilicate melts near minimum liquidus temperature. Physical Chemistry Chemical Physics, 2015, 17, 9313-9325.	1.3	11
74	Simultaneous CVD Growth of Nanostructured Carbon Hybrids. NATO Science for Peace and Security Series A: Chemistry and Biology, 2015, , 111-117.	0.5	0
75	Dielectric characterization of low-loss calcium strontium titanate fibers produced by laser floating zone technique for wireless communication. Physica Status Solidi (A) Applications and Materials Science, 2014, 211, 2086-2089.	0.8	0
76	Stiff Diamond/Buckypaper Carbon Hybrids. ACS Applied Materials & Interfaces, 2014, 6, 22649-22654.	4.0	12
77	ZnO micro/nanocrystals grown by laser assisted flow deposition. , 2014, , .		1
78	Role of high microwave power on growth and microstructure of thick nanocrystalline diamond films: A comparison with large grain polycrystalline diamond films. Journal of Crystal Growth, 2014, 389, 83-91.	0.7	11
79	Development of a new thermoelectric Bi2Ca2Co1.7Ox+Ca3Co4O9 composite. Scripta Materialia, 2014, 80, 1-4.	2.6	14
80	Mechanical behaviour of zirconia–mullite directionally solidified eutectics. Materials & Design, 2014, 61, 211-216.	5.1	25
81	Ionic conductivity of directionally solidified zirconia–mullite eutectics. Solid State Ionics, 2014, 256, 45-51.	1.3	5
82	Directional solidification of ZrO2–BaZrO3 composites with mixed protonic–oxide ionic conductivity. Solid State Ionics, 2014, 262, 654-658.	1.3	4
83	Effects of Mn doping on the electrical and dielectric properties of CaCu 3 Ti 4 O 12 fibres. Ceramics International, 2014, 40, 16503-16511.	2.3	25
84	Effects of transition metal additives on redox stability and high-temperature electrical conductivity of (Fe,Mg)3O4 spinels. Journal of the European Ceramic Society, 2014, 34, 2339-2350.	2.8	12
85	Synthesis of Long ZnO Nanorods under Microwave Irradiation or Conventional Heating. Journal of Physical Chemistry C, 2014, 118, 14629-14639.	1.5	120
86	Crystallization of iron-containing Si–Al–Mg–O glasses under laser floating zone conditions. Journal of Alloys and Compounds, 2014, 611, 57-64.	2.8	12
87	Effect of Current Polarity on BSCCO/Ag Ceramics Textured by Electrically Assisted Laser Floating Zone. Journal of Superconductivity and Novel Magnetism, 2013, 26, 943-946.	0.8	26
88	Directionally solidified eutectic and off-eutectic mullite–zirconia fibres. Journal of the European Ceramic Society, 2013, 33, 953-963.	2.8	17
89	Redox stability and high-temperature electrical conductivity of magnesium- and aluminium-substituted magnetite. Journal of the European Ceramic Society, 2013, 33, 2751-2760.	2.8	12
90	NbO/Nb2O5 core–shells by thermal oxidation. Journal of the European Ceramic Society, 2013, 33, 3077-3083.	2.8	11

#	Article	IF	CITATIONS
91	The influence of photon excitation and proton irradiation on the luminescence properties of yttria stabilized zirconia doped with praseodymium ions. Nuclear Instruments & Methods in Physics Research B, 2013, 306, 207-211.	0.6	2
92	Magnetite/hematite core/shell fibres grown by laser floating zone method. Applied Surface Science, 2013, 278, 203-206.	3.1	13
93	Optical and dielectric behaviour of EuNbO4 crystals. Journal of Materials Chemistry C, 2013, 1, 2913.	2.7	30
94	Prospects on laser processed wide band gap oxides optical materials. Proceedings of SPIE, 2013, , .	0.8	2
95	Microprobe analysis, iono- and photo-luminescence of Mn2+ activated ZnGa2O4 fibres. Nuclear Instruments & Methods in Physics Research B, 2013, 306, 195-200.	0.6	12
96	Preparation of high-performance Ca3Co4O9 thermoelectric ceramics produced by a new two-step method. Journal of the European Ceramic Society, 2013, 33, 1747-1754.	2.8	73
97	Towards the understanding of the intentionally induced yellow luminescence in GaN nanowires. Physica Status Solidi C: Current Topics in Solid State Physics, 2013, 10, 667-672.	0.8	8
98	Spectroscopic studies of Tm-doped zirconia nanoparticles. Physica Status Solidi (B): Basic Research, 2013, 250, 815-820.	0.7	8
99	Laser Melting Processing of ZrO <sub>2</sub> –BaZrO <sub>3</sub> Ceramic Eutectics. Science of Advanced Materials, 2013, 5, 1847-1856.	0.1	3
100	Ionic conductivity of eutectic mullite-zirconia fibres. , 2012, , .		0
101	ZnO Nano/Microstructures Grown by Laser Assisted Flow Deposition. Journal of Nano Research, 2012, 18-19, 129-137.	0.8	11
102	Quantification of Microstructural Features in Carbon Nanotube/Nanodiamond Hybrids. Microscopy and Microanalysis, 2012, 18, 85-86.	0.2	0
103	ZnGa2O4:Mn2+ Phosphors Grown by Laser Floating Zone. Microscopy and Microanalysis, 2012, 18, 105-106.	0.2	0
104	Laser Assisted Flow Deposition: a New Method to Grow ZnO. Microscopy and Microanalysis, 2012, 18, 87-88.	0.2	2
105	Electrical Polarization Effect on Bi2Ca2Co1.7Ox thermoelectrics grown by laser floating zone. Microscopy and Microanalysis, 2012, 18, 93-94.	0.2	5
106	Exotic Manganese Dioxide Structures in Niobium Oxides Capacitors. Microscopy and Microanalysis, 2012, 18, 99-100.	0.2	5
107	Microstructure of Mullite-zirconia Fibres Grown by Directional Solidification. Microscopy and Microanalysis, 2012, 18, 103-104.	0.2	0
108	Dielectric properties and microstructure of CaCu <inf>3</inf> Ti <inf>4−x</inf> Mn <inf>x</inf> 0 <inf>12</inf> fibres grown by laser floating zone technique. , 2012, , .		0

#	Article	IF	CITATIONS
109	ZnO nanostructures grown on vertically aligned carbon nanotubes by laser-assisted flow deposition. Acta Materialia, 2012, 60, 5143-5150.	3.8	24
110	Optical properties of LFZ grown β-Ga2O3:Eu3+ fibres. Applied Surface Science, 2012, 258, 9157-9161.	3.1	28
111	Lithium niobate bulk crystallization promoted by CO2 laser radiation. Applied Surface Science, 2012, 258, 9457-9460.	3.1	10
112	Structural, optical and magnetic resonance properties of TiO2 fibres grown by laser floating zone technique. Applied Surface Science, 2012, 258, 9143-9147.	3.1	13
113	Enhancement of superconductivity in LFZ-grown BSCCO fibres by steeper axial temperature gradients. Applied Surface Science, 2012, 258, 9175-9180.	3.1	16
114	New method to improve the grain alignment and performance of thermoelectric ceramics. Materials Letters, 2012, 83, 144-147.	1.3	53
115	Red light from ZrO2:Eu3+ nanostructures. Materials Science and Engineering B: Solid-State Materials for Advanced Technology, 2012, 177, 712-716.	1.7	36
116	Synthesis, structural and optical characterization of ZnO crystals grown in the presence of silver. Thin Solid Films, 2012, 520, 4717-4721.	0.8	14
117	Sintered NbO Powders for Electronic Device Applications. Journal of Physical Chemistry C, 2011, 115, 4879-4886.	1.5	61
118	YSZ:Dy3+ single crystal white emitter. Journal of Materials Chemistry, 2011, 21, 15262.	6.7	45
119	Red and infrared luminescence from tetragonal YSZ:Pr3+ single crystal fibres grown by LFZ. Optical Materials, 2011, 34, 27-29.	1.7	11
120	Bright room-temperature green luminescence from YSZ:Tb3+. Materials Letters, 2011, 65, 1979-1981.	1.3	24
121	Colossal dielectric constant of poly- and single-crystalline CaCu3Ti4O12 fibres grown by the laser floating zone technique. Acta Materialia, 2011, 59, 102-111.	3.8	27
122	Electrical assisted laser floating zone (EALFZ) growth of 2212-BSCCO superconducting fibres. Applied Surface Science, 2011, 257, 5283-5286.	3.1	13
123	Effect of processing method on physical properties of Nb2O5. Journal of the European Ceramic Society, 2011, 31, 501-506.	2.8	61
124	Effect of microwave power and nitrogen addition on the formation of {100} faceted diamond from microcrystalline to nanocrystalline. Vacuum, 2011, 85, 1130-1134.	1.6	21
125	Structural and optical properties of europium doped zirconia single crystals fibers grown by laser floating zone. Journal of Applied Physics, 2011, 109, .	1.1	38
126	Effect of Eu2O3 doping on Ta2O5 crystal growth by the laser-heated pedestal technique. Journal of Crystal Growth, 2010, 313, 62-67.	0.7	7

#	Article	IF	CITATIONS
127	Single and polycrystalline mullite fibres grown by laser floating zone technique. Journal of the European Ceramic Society, 2010, 30, 3311-3318.	2.8	20
128	The role of surface activation prior to seeding on CVD diamond adhesion. Surface and Coatings Technology, 2010, 204, 3585-3591.	2.2	15
129	Characterisation of interface formed at 650°C between AISI H13 steel and Al–12Si–1Cu aluminium melt. International Journal of Cast Metals Research, 2010, 23, 231-239.	0.5	7
130	From Micro to Nanometric Grain Size CVD Diamond Tools. Materials Research Society Symposia Proceedings, 2009, 1243, 1.	0.1	1
131	Pulling rate and current intensity competition in an electrically assisted laser floating zone. Superconductor Science and Technology, 2009, 22, 065016.	1.8	11
132	Radial inhomogeneities induced by fiber diameter in electrically assisted LFZ growth of Bi-2212. Applied Surface Science, 2009, 255, 5503-5506.	3.1	14
133	Surface activation pre-treatments for NCD films grown by HFCVD. Vacuum, 2009, 83, 1228-1232.	1.6	13
134	Structure and morphology of TiB2 duplex coatings deposited over X40 CrMoV 5-1-1 steel by DC magnetron sputtering. Vacuum, 2009, 83, 1291-1294.	1.6	5
135	Structural and optical properties on thulium-doped LHPG-grown Ta2O5 fibres. Microelectronics Journal, 2009, 40, 309-312.	1.1	10
136	Nano carbon hybrids from the simultaneous synthesis of CNT/NCD by MPCVD. Diamond and Related Materials, 2009, 18, 160-163.	1.8	13
137	CVD micro/nanocrystalline diamond (MCD/NCD) bilayer coated odontological drill bits. Diamond and Related Materials, 2009, 18, 264-270.	1.8	41
138	Adhesion and Wear Behaviour of NCD Coatings on Si <sub>3</sub> N <sub>4</sub> by Micro-Abrasion Tests. Journal of Nanoscience and Nanotechnology, 2009, 9, 3938-3943.	0.9	12
139	Electric field-modified segregation in crystal fibers of colossal magnetoresistive La0.7Ca0.3MnO3. Journal of Crystal Growth, 2008, 310, 3568-3572.	0.7	6
140	Microwave dielectric permittivity and photoluminescence of Eu2O3 doped laser heated pedestal growth Ta2O5 fibers. Applied Physics Letters, 2008, 92, 252904.	1.5	6
141	Nucleation of nanocrystalline diamond on masked/unmasked Si3N4 ceramics with different mechanical pretreatments. Diamond and Related Materials, 2008, 17, 440-445.	1.8	8
142	Biocompatibility evaluation of DLC-coated Si3N4 substrates for biomedical applications. Diamond and Related Materials, 2008, 17, 878-881.	1.8	73
143	Nano- and micro-crystalline diamond growth by MPCVD in extremely poor hydrogen uniform plasmas. Diamond and Related Materials, 2007, 16, 757-761.	1.8	29
144	Deposition of TiB2 onto X40 CrMoV 5-1-1 steel substrates by DC magnetron sputtering. Vacuum, 2007, 81, 1519-1523.	1.6	8

#	Article	IF	CITATIONS
145	Room temperature PL characterization of micro and nanocrystalline diamond grown by MPCVD from Ar/H2/CH4 mixtures. Vacuum, 2007, 81, 1416-1420.	1.6	5
146	Critical current density improvement in BSCCO superconductors by application of an electric current during laser floating zone growth. Physica C: Superconductivity and Its Applications, 2007, 460-462, 1347-1348.	0.6	11
147	Vortex dimensionality and pinning efficiency in granular specimens having a narrow weak-link critical current distribution. Journal of Physics: Conference Series, 2006, 43, 618-622.	0.3	0
148	Hard a-C/DLC coatings on Si3N4–bioglass composites. Diamond and Related Materials, 2006, 15, 944-947.	1.8	4
149	Annealing time effect on Bi-2223 phase development in LFZ and EALFZ grown superconducting fibres. Applied Surface Science, 2006, 252, 4957-4963.	3.1	5
150	NCD by HFCVD on a Si3N4-bioglass composite for biomechanical applications. Surface and Coatings Technology, 2006, 200, 6409-6413.	2.2	7
151	Reciprocating sliding behaviour of self-mated amorphous diamond-like carbon coatings on Si3N4 ceramics under tribological stress. Thin Solid Films, 2006, 515, 2192-2196.	0.8	1
152	Enhancement of Bi-2223 phase formation by electrical assisted laser floating zone technique. Journal of Physics and Chemistry of Solids, 2006, 67, 416-418.	1.9	3
153	The effect of current direction on superconducting properties of BSCCO fibres grown by an electrically assisted laser floating zone process. Superconductor Science and Technology, 2006, 19, 15-21.	1.8	6
154	Bi–Sr–Ca–Cu–O superconducting fibres processed by the laser floating zone technique under different electrical current intensities. Superconductor Science and Technology, 2006, 19, 373-380.	1.8	6
155	The Effect of Annealing Temperature on the Transport Properties of BSCCO Fibres Grown by LFZ and EALFZ. Materials Science Forum, 2006, 514-516, 338-342.	0.3	1
156	Preparation and Properties of New Superconductor Material MgB <sub>2</sub> . Materials Science Forum, 2006, 514-516, 333-337.	0.3	0
157	Unstressed PACVD diamond films on steel pre-coated with a composite multilayer. Surface and Coatings Technology, 2005, 191, 102-107.	2.2	16
158	Directly MPCVD diamond-coated Si3N4 disks for dental applications. Diamond and Related Materials, 2005, 14, 626-630.	1.8	1
159	Cutting of Free Standing CVD Diamond Films by Optical Fibre Guided Nd:YAG Laser. Materials Science Forum, 2004, 455-456, 614-618.	0.3	0
160	Hot-filament chemical vapour deposition of nanodiamond on silicon nitride substrates. Diamond and Related Materials, 2004, 13, 643-647.	1.8	32
161	LFZ fibre texture modification induced by electrical polarization. Physica C: Superconductivity and Its Applications, 2004, 408-410, 915-916.	0.6	10
162	Textured Bi–Sr–Ca–Cu–O rods processed by laser floating zone from solid state or melted precursors. Physica C: Superconductivity and Its Applications, 2004, 415, 163-171.	0.6	35

#	Article	IF	CITATIONS
163	Mechanical properties evaluation of fluor-doped diamond-like carbon coatings by nanoindentation. Thin Solid Films, 2004, 446, 85-90.	0.8	27
164	A new interlayer approach for CVD diamond coating of steel substrates. Diamond and Related Materials, 2004, 13, 828-833.	1.8	42
165	Electrical field freezing effect on laser floating zone (LFZ)-grown Bi2Sr2Ca2Cu4O11superconducting fibres. Superconductor Science and Technology, 2004, 17, 612-619.	1.8	24
166	Si <sub>3</sub> N <sub>4</sub> recubierto con diamante CVD mediante filamento caliente y plasma generado por microondas. Boletin De La Sociedad Espanola De Ceramica Y Vidrio, 2004, 43, 473-476.	0.9	1
167	Tribological behaviour of CVD diamond films on steel substrates. Wear, 2003, 255, 846-853.	1.5	34
168	On the half unit cell intergrowth of Bi2Sr2Ca3Cu4O12 with other superconducting phases in two-step annealed LFZ fibres. Physica C: Superconductivity and Its Applications, 2003, 398, 31-36.	0.6	7
169	Surface Pretreatments of Silicon Nitride for CVD Diamond Deposition. Journal of the American Ceramic Society, 2003, 86, 749-754.	1.9	20
170	Acoustic emission detection of macro-indentation cracking of diamond coated silicon. Diamond and Related Materials, 2003, 12, 1744-1749.	1.8	2
171	Adhesion behaviour assessment on diamond coated silicon nitride by acoustic emission. Diamond and Related Materials, 2003, 12, 733-737.	1.8	50
172	Wear resistant CVD diamond tools for turning of sintered hardmetals. Diamond and Related Materials, 2003, 12, 738-743.	1.8	39
173	Tailored Si3N4Ceramic Substrates for CVD Diamond Coating. Surface Engineering, 2003, 19, 410-416.	1.1	20
174	Trapping control of phase development in zone melting of BiÂSrÂCaÂCuÂO superconducting fibres. Superconductor Science and Technology, 2003, 16, 392-397.	1.8	7
175	Microwave plasma chemical vapour deposition diamond nucleation on ferrous substrates with Ti and Cr interlayers. Diamond and Related Materials, 2002, 11, 1617-1622.	1.8	58
176	Abrasive Resistance of CVD Diamond Brazed Thick Films in Machining of WC Pre-Sintered Forms. Key Engineering Materials, 2002, 230-232, 193-198.	0.4	2
177	Thermal conductivity enhancement in cutting tools by chemical vapor deposition diamond coating. Diamond and Related Materials, 2002, 11, 703-707.	1.8	25
178	On the Half Unit Cell Intergrowth of Bi2Sr2Ca3Cu4Ox with Other Superconducting Phases in Two-step Annealed LFZ Fibers. Microscopy and Microanalysis, 2002, 8, 1352-1353.	0.2	0
179	Effect of intergranular phase of Si3N4 substrates on MPCVD diamond deposition. Surface and Coatings Technology, 2002, 151-152, 521-525.	2.2	6
180	Wettability studies of reactive brazing alloys on CVD diamond plates. Diamond and Related Materials, 2001, 10, 775-780.	1.8	25

#	Article	IF	CITATIONS
181	MPCVD diamond tool cutting-edge coverage: dependence on the side wedge angle. Diamond and Related Materials, 2001, 10, 803-808.	1.8	20
182	Growth of the Bi-2223 phase after a short nucleation stage at high temperature. Physica B: Condensed Matter, 2001, 294-295, 700-704.	1.3	3
183	Title is missing!. Journal of Materials Science: Materials in Electronics, 2001, 12, 269-271.	1.1	16
184	Diffusion phenomena and crystallization path during the growth of LFZ Bi-Sr-Ca-Cu-O superconducting fibres. Superconductor Science and Technology, 2001, 14, 910-920.	1.8	23
185	Influence of SiC particle addition on the nucleation density and adhesion strength of MPCVD diamond coatings on Si 3 N 4 substrates. Diamond and Related Materials, 2000, 9, 483-488.	1.8	20
186	Phase transformation kinetics during thermal annealing of LFZ Bi–Sr–Ca–Cu–O superconducting fibers in the range 800–870°C. Physica C: Superconductivity and Its Applications, 1999, 323, 23-41.	0.6	34
187	Crystallization process, phase chemistry and transport properties of superconducting fibers prepared by the LFZ method followed by isothermal annealing. Physica C: Superconductivity and Its Applications, 1994, 235-240, 513-514.	0.6	5
188	Bi-Ca-Sr-Cu-O superconductors obtained by glass crystallisation; Effect of potassium doping. Physica C: Superconductivity and Its Applications, 1989, 159, 273-276.	0.6	2
189	Preparation of superconductors of the BiSrCaCuO system by glass crystallization. Journal of the Less Common Metals, 1989, 150, 305-310.	0.9	4